

1 **Temperature and hydrological variations during the Late-Glacial in the central**
2 **Mediterranean: application of the novel ostracod-clumped thermometer.**

3

4 Marchegiano Marta^{1,2*}, Peral Marion^{2,3}, Doyle Rebecca², García-Alix Antonio¹, Francke
5 Alexander^{4,5}, Snoeck Christophe², Goderis Steven², and Claeys Philippe²

6

7 *1: Departamento de Estratigrafía y Paleontología, Universidad de Granada, 18071 Granada, España; martamarchegiano@ugr.es,
8 agalix@ugr.es.*

9 *2: Archaeology, Environmental changes and Geo-Chemistry, Vrije Universiteit Brussel, Pleinlaan 2, 1050 Brussel, Belgium.*
10 *marion.peral@vub.be; rebecca.doyle@vub.be; christophe.snoeck@vub.be; steven.goderis@vub.be; phclaeys@vub.be.*

11 *3: Environnements et Paléoenvironnements Océaniques et Continentaux (EPOC), Univ. Bordeaux, CNRS, Bordeaux INP, EPOC, UMR 5805,*
12 *F-33600 Pessac, France*

13 *4: Archeology, College of Humanities, Arts and Social Science, Flinders University, 5042 Adelaide, Australia;*
14 *alexander.francke@flinders.edu.au*

15 *5: School of Physics, Chemistry and Earth Sciences, Faculty of Sciences, Engineering and Technology, The University of Adelaide, 5005*
16 *Adelaide, Australia*

17 **Corresponding author: Marta Marchegiano, martamarchegiano@ugr.es*

18 **STATEMENT**

19 This manuscript has been submitted for publication in Earth and Planetary Science Letter.
20 Please note that, despite having undergone peer-review, the manuscript is still not accepted for
21 publication. Subsequent versions of this manuscript may have slightly different content. If
22 accepted, the final version of this manuscript will be available via the 'Peer-reviewed
23 Publication DOI' link on the right-hand side of this webpage.

24

25 Twitter account: @MaMarchegiano

26 **Temperature and hydrological variations during the Late-Glacial in the central**
27 **Mediterranean: application of the novel ostracod-clumped thermometer.**

28

29 Marchegiano Marta^{1,2*}, Peral Marion^{2,3}, Doyle Rebecca², García-Alix Antonio¹, Francke
30 Alexander^{4,5}, Snoeck Christophe², Goderis Steven², and Claeys Philippe²

31

32 *1: Departamento de Estratigrafía y Paleontología, Universidad de Granada, 18071 Granada, España*

33 *2: Archaeology, Environmental changes and Geo-Chemistry, Vrije Universiteit Brussel, Pleinlaan 2, 1050 Brussel, Belgium*

34 *3: Environnements et Paléoenvironnements Océaniques et Continentaux (EPOC), Univ. Bordeaux, CNRS, Bordeaux INP, EPOC, UMR 5805,*

35 *F-33600 Pessac, France*

36 *4: Archeology, College of Humanities, Arts and Social Science, Flinders University, 5042 Adelaide, Australia*

37 *5: School of Physics, Chemistry and Earth Sciences, Faculty of Sciences, Engineering and Technology, The University of Adelaide, 5005*

38 *Adelaide, Australia*

39 **Corresponding author: Marta Marchegiano*

40

41 **ABSTRACT**

42

43 In this study we show, for the first time, the absence of a vital effect in the clumped isotope
44 carbonate (Δ_{47}) fossil ostracod signal, as well as the ability of the novel ostracod- Δ_{47}
45 thermometer to reconstruct past hydrological conditions in complex lacustrine systems.
46 Furthermore, through the application of Δ_{47} analyses on the ostracod species *Candona angulata*
47 and *Cyprideis torosa* from Lake Trasimeno record (central Italy), which today precipitate their
48 shells during the cold and the warm season respectively, we provide evidence that by
49 combining biological (i.e., ostracod shell precipitation timing), paleontological (i.e.,
50 identification of ostracod species) and geochemical (i.e., Δ_{47}) approaches, the ostracod- Δ_{47}

51 thermometer can be used to accurately reconstruct past seasonality. This also implies that,
52 despite the absence of a vital effect, not all species can be combined for Δ_{47} analyses in
53 environments with seasonal temperature variations; rather, only those that precipitate their
54 shells during the same season should be considered. The application of the ostracod- Δ_{47}
55 thermometer on the Trasimeno lacustrine record gives rise to the first continental warm season
56 paleotemperature reconstruction of the last 43 ky in central Mediterranean area. The
57 combination of Δ_{47} and classic stable isotope ($\delta^{18}\text{O}_{\text{ost}}$) measured on ostracod shells provides
58 the isotopic composition of the water from which the carbonate precipitated ($\delta^{18}\text{O}_{\text{w}}$) and
59 thereby, changes in the evaporation/precipitation balance in this area. Before the Last Glacial
60 Maximum (LGM), equivalent to the Marine Isotopic Stage 3 (MIS3, from 43 to 29ky), warm
61 season temperatures ranged from 15 ± 1.6 °C to 22 ± 2.3 °C, being from 2 to 6 °C colder than
62 today. Hydrological conditions during this period were similar to the present-day ones,
63 characterized by a permanent lake and a high evaporation/precipitation ratio (E/P). The drastic
64 decrease of the warm season temperatures (ranging from 10 ± 2.9 °C to 17 ± 3.1 °C) and of the
65 E/P ratio during LGM and Lateglacial (MIS2, from 29 to 11.6 ky) corresponded well to the
66 global climate cooling and low summer insolation, suggesting an amplifying role, of this last
67 one, in the effects of the millennial scale climatic variations. At the Pleistocene/Holocene
68 transition, both warm season temperature (25 ± 2 °C) and the E/P ratio increased in conjunction
69 with the summer insolation. During the early Holocene, warm season temperature (23 ± 2 °C)
70 closely resemble present-day values. However, cold season temperatures (12 ± 2 °C) were
71 approximately 4 °C warmer than today. Notably, no hydrological differences were identified
72 between the warm and the cold season underlying a lower seasonality contrast compared to the
73 present, along with enhanced warm season precipitation. The good agreement between the Δ_{47}
74 temperatures reconstructed for the last 1 ky and the temperatures presently recorded at Lake

75 Trasimeno (8 °C cold and 22 °C for warm season), confirms the accuracy of the analyses and
76 the applicability of the ostracod- Δ_{47} thermometer to reconstruct seasonal temperature changes.

77

78 **KEYWORDS**

79 Carbonate Clumped Isotope, Freshwater ostracods, Paleotemperatures, Paleohydrology,
80 Seasonality, Central Mediterranean.

81

82 **1. INTRODUCTION**

83

84 The Intergovernmental Panel on Climate Change (IPCC) considers the Mediterranean region a
85 climate change hotspot (Ali et al., 2022). According to climate projections, the Mediterranean
86 region is expected to warm at a rate approximately 20% higher than the global average.

87 Additionally, it will undergo significant drying, a phenomenon not anticipated in other regions
88 situated at the same latitude (Lionello and Scarascia, 2018; Saeger et al., 2014). The
89 vulnerability of this area is a consequence of complex and interacting processes related to the
90 area's landscapes, geographical location, high population density, and long history of human
91 occupation (Ali et al., 2022).

92 Predictive modelling of potential future climate scenarios is key to developing strategies for
93 adaptation and mitigation. To generate these climate projections, the forcing mechanisms
94 driving climate variability across different temporal and geographical scales need to be better
95 understood. Also, the modelling of forecasted changes with ancient analogues must be
96 validated. Owing to the Mediterranean's complex topography, each region responds
97 differently to atmospheric and marine climate dynamics (Abrantes et al., 2012). Accurate high-
98 resolution paleoclimatic reconstructions for the different Mediterranean regions are thus
99 required. Lake sediments are certainly among the best continental archives for developing

100 paleoclimatic and paleoenvironmental reconstructions because they can capture rapid climate
101 changes across regional scales (Gornitz, 2009; Cohen, 2003). Paleotemperature reconstructions
102 have always been assumed to play an important role in understanding climatic variations;
103 however, despite more than half a century of studies, quantitative and well-constrained
104 temperature reconstruction remains very challenging. The complexity lies in disentangling and
105 quantifying the effects of the various parameters that impact on the local climate and
106 environment (e.g., temperature, hydrology, lake structure). Continental quantitative
107 temperature records in the central Mediterranean area are very rare, mainly focussed on the last
108 15 ky (Heiri et al., 2015; Larocque and Finsinger, 2008; Robles et al., 2023; Samartin et al.,
109 2017) and most of them are based on transfer functions (e.g, pollen, chironomids, and
110 ostracods). The oldest temperature record comes from the Monticchio lake (southern Italy,
111 Fig.1). It is based on pollen analyses, and provides air temperature of the coldest month
112 (January) from the last ca. 102 ky (Allen et al., 1999). Marchegiano et al., (2020) applied the
113 Mutual Ostracod Temperature Range transfer function (MOTR, Horne, 2007) to ostracod
114 assemblages from Lake Trasimeno (central Italy, Fig.1) to reconstruct air temperature of the
115 warmest (July) and coldest (January) months during the Late Pleistocene. However, this
116 approach produced very large temperature ranges within which the real temperature existed
117 (Marchegiano et al., 2020, Fig. 3).

118 The carbonate clumped isotope (Δ_{47}) technique (Eiler, 2007), currently mostly applied to
119 marine carbonate fossils and sediments (de Winter et al., 2021; Henkes et al., 2013;
120 Marchegiano and John, 2022; Meinicke et al., 2021; Peral et al., 2020), has the potential to
121 significantly reduce the methodological uncertainties associated with lake paleotemperature
122 measurements. This technique is based on the temperature-dependent abundance of ^{13}C - ^{18}O
123 bonds in carbonate CO_2 . The increased abundance of these bonds in carbonate is associated
124 with decreasing water temperatures, revealing the temperatures at which calcium carbonate

125 (CaCO₃) precipitated. The combination of Δ_{47} and $\delta^{18}\text{O}$ provide the $\delta^{18}\text{O}_w$ and give insight on
126 the hydrological conditions.

127 The ostracod- Δ_{47} thermometer is a new tool able to reconstruct lacustrine water temperatures,
128 with an accuracy of $\sim \pm 2$ °C (Marchegiano et al., in review). Marchegiano et al. (in review),
129 showed the applicability of the Δ_{47} technique on ostracod shells as well as the absence of any
130 vital effect (i.e., disequilibrium between the water isotopic signal and the one recorded by the
131 organisms) on ostracods living at the same temperatures. Ostracods are aquatic micro-
132 crustaceans (size from 0.3 to 5 mm) with a stable bivalve low-Mg calcite shells easily to
133 preserve and thus ideally suited for geochemical analyses (Holmes and De Deckker, 2012). As
134 they grow, they secrete increasingly large carapaces from the ions dissolved in the host water
135 and pass through 8 molting stages before reaching adulthood (Turpen and Angell, 1971). The
136 shell calcification is quick, ranging from a few hours to a few days (Börner et al., 2013), and
137 representative of the geochemical conditions of the environment at that time (Chivas et al.,
138 1983; Mischke et al., 2010; Pérez et al., 2011).

139 In this study, we generated the first ca. 43 ky continental warm season temperature record for
140 the central Mediterranean area by applying the novel ostracod- Δ_{47} thermometer (Marchegiano
141 et al., in review) on a ca. 8.9 m long sedimentary core from Lake Trasimeno (central Italy).
142 The Trasimeno sedimentary core has been well analyzed in previous studies (Francke et al.,
143 2021; Gasperini et al., 2022; Marchegiano et al., 2020, 2019, 2018) by using a multiproxy
144 approach (i.e., micropaleontological, sedimentological and geochemical) making this record
145 particularly suitable for the application of this novel paleothermometer.

146 The clumped isotope technique has already been applied on fossil ostracods to reconstruct
147 paleoaltitude (Song et al., 2022) and paleotemperatures (Yue et al., 2022); however, no studies
148 have ever determined whether a vital effect influences the Δ_{47} signal on fossil ostracods. To fill
149 this gap, we performed Δ_{47} analyses on two different ostracod species coming from the same

150 sample that lived and precipitated their shells at the same season and temperatures. Also, by
151 combining Δ_{47} with the analyses of the classic oxygen isotopic composition of the ostracod
152 shells ($\delta^{18}\text{O}_{\text{ost}}$), we show, for the first time, the ability of the ostracod- Δ_{47} thermometer to
153 reconstruct $\delta^{18}\text{O}_{\text{w}}$ variations in past lacustrine environments.

154

155 **1.1 Study site: Lake Trasimeno**

156

157 Lake Trasimeno (latitude 43°08'N, longitude 12°06'E, 258 m above sea level, Fig. 2) is an
158 endorheic and very shallow lake (max depth of ~6 m and ~4 m in average) with a surface area
159 of 124.3 km² located in central Italy (Umbria region). It has a tectonic origin and the lacustrine
160 sedimentation started during the Middle Pleistocene (Gasperini et al., 2010). Because of its
161 characteristics, the hydrology of the lake strictly depends on climatic and environmental
162 variations. Lake-level fluctuations influence, at the seasonal and annual-decadal scale, the
163 physical-chemical and biological lake properties (Ludovisi and Gaino, 2010; Marchegiano et
164 al., 2017; Pallottini et al., 2023). The climate regime is characterized by warm-arid summers
165 and mild-humid winters. Today, water temperatures are close to the atmospheric ones with a
166 difference of 2 - 4 °C during the year. Temperatures are homogeneous along the entire water
167 column due to a continuous mixing facilitated by the shallowness and the very large surface of
168 the lake (Marchegiano et al., 2017). Previous studies (Marchegiano et al., 2018, 2019, 2020
169 and Francke et al., 2022) showed that, over the last ca. 47 ky, Lake Trasimeno responded
170 rapidly to millennial scale climatic variations associated with Greenland stadial and interstadial
171 events, according to Rasmussen et al., (2016). Low (high) lake levels corresponded to cold
172 (warm) and dry (humid) stadial (interstadial) events. This demonstrates that Lake Trasimeno
173 detects regional as well as global climatic signals. The living and fossil ostracod fauna of Lake
174 Trasimeno have also been studied intensively (Marchegiano et al., 2017, 2018, 2019 and 2020),

175 indicating a prevalence of permanent low saline lake conditions during MIS3 and the Holocene
176 and ephemeral high salinity lake conditions during the MIS2.

177 Thanks to its strategical position in the central Mediterranean, its high sensitivity to climate
178 and environmental changes and the abundance and great preservation of the ostracod fauna,
179 Lake Trasimeno is the perfect target to test the ostracod- Δ_{47} thermometer in past sedimentary
180 records and to reconstruct atmospheric changes in the central Mediterranean.

181

182 **2. Material and Methods**

183

184 **2.1 Trasimeno core and its chronology**

185

186 An 8.6 m long sediment core (Co1320; 43° 09.624'N, 12° 03.491'E) (Fig. 2) was retrieved at
187 ~4.9 m water depth from a floating platform using a gravity piston corer (UWITEC®) during
188 a sampling campaign in November 2014. The core was split lengthwise in the laboratory. While
189 one-half was archived and stored at the University of Cologne (Germany), the other half was
190 used for visual lithological inspection and then subsampled at 2-cm intervals for geochemical
191 and micropalaeontological analyses (Marchegiano et al., 2018, 2019, 2020 and Francke et al.,
192 2022).

193 The chronological model of the Trasimeno core Co1320 has been developed using ten
194 radiocarbon ages (Fig. 3) and ultimately covers the last ca. 47 ky (Marchegiano et al., 2018).

195 In this study, we updated this calibration using a Bayesian age-depth modelling calculated by
196 means of the software rBacon 3.1 (Blaauw et al., 2018; Blaauw and Christen, 2011), and the
197 IntCal 2020 calibration curve (Reimer, 2020) (Fig. 3). The bulk organic matter samples at 631
198 cm (COL3665.1.1) and 154.5 cm (COL3662.1.1) exhibit higher $br/(cren+cren0)$ GDGT ratios,
199 indicating a substantial contribution from soli organic matter (SOM) (Francke et al., 2022).

200 This implies that the incorporation of pre-aged SOM in these samples may distort the bulk ^{14}C
201 age. Consequently, the two samples were excluded from the age-depth model. Considering the
202 limited presence of carbonate bedrock in the catchment area and the high lake surface compared
203 to the water volume ratio, that facilitate rapid exchange with the atmosphere, Lake Trasimeno
204 is anticipated to have minimal reservoir and/or hardwater effects on lacustrine organic matter
205 (Francke et al., 2022).

206

207 **2.2 Carbonate classic and clumped-isotope analyses**

208

209 For classic and clumped-isotope analyses, we selected a total of 16 samples (Table 1) by
210 combining the results of the ostracod assemblage analyses (Marchegiano et al., 2018 and 2019),
211 the derived MOTR temperature curve (Marchegiano et al., 2020) and the updated age model.
212 These samples correspond to the main temperature and environmental variations along the
213 entire core interval. To reach the required carbonate amount for clumped-isotope analyses
214 (minimum 500 μg per replicate), we merged adjacent subsamples (2 cm thick) (Table 1)
215 deposited during the same climatic event (Marchegiano et al., 2018, 2019 and 2020). Adult
216 ostracod shells were picked and manually cleaned with a brush under the stereomicroscope to
217 remove any sediments and other possible contaminants (i.e., organic matter). The good state of
218 preservation (i.e., no diagenetic alteration) of the ostracod shells was checked under the
219 scanning electron microscope (SEM) (Figure 4). Analyses for Δ_{47} and $\delta^{18}\text{O}_{\text{ost}}$ were carried out
220 on the most abundant species *Cyprideis torosa*, *Sarocypridopsis aculeata*, *Eucypris mareotica*,
221 *Heterocypris salina* and *Candona angulata* (Figure 4). A total of 40 to 60 valves per replicate
222 is needed to assure sufficient material (500 - 600 μg per replicate), whereby the exact number
223 depends on the species (i.e., size and thickness of the shells). Each sample is replicated from 5
224 to 15 times (300 - 1000 valves per samples in total). The Δ_{47} analyses of ostracod shells, which

225 provide at the same time the $\delta^{18}\text{O}_{\text{ost}}$ data, were carried out at the Analytical, Environmental &
226 Geo-Chemistry (AMGC) clumped isotope lab of the Vrije Universiteit Brussel (VUB), using
227 a Nu Instruments Perspective-IS stable isotope ratio mass spectrometer (SIRMS) in
228 conjunction with a Nu-Carb carbonate sample preparation system, as described in detail in De
229 Vleeschouwer et al., (2022). The analyses were performed between March 2022 and November
230 2022. The carbonate standard ETH-4 was systematically measured and compared to InterCarb
231 values (Bernasconi et al., 2021) to assess the accuracy and reproducibility. Analyses and results
232 were monitored in the lab using the Easotope software (John and Bowen, 2016). Within the
233 ClumpyCrunch software (Daëron, 2021), the raw measured Δ_{47} values were processed using
234 the IUPAC Brand's isotopic parameters (Daëron et al., 2016) and converted to the ICDES 90°C
235 scale, using the most recent values for the ETH-1, ETH-2, and ETH-3 carbonate reference
236 materials (Bernasconi et al., 2021). Analytical and calibration uncertainties were propagated to
237 calculate the final uncertainties on temperatures. The Δ_{47} values were converted into
238 temperatures using the unified calibration (Anderson et al., 2021) as suggested by
239 (Marchegiano et al., in review) and the $\delta^{18}\text{O}_{\text{w}}$ values were calculated from Δ_{47} and $\delta^{18}\text{O}_{\text{ost}}$ data
240 using the formula of (Kim and O'Neil, 1997) for calcite (Table 1). Since the $\delta^{18}\text{O}_{\text{ost}}$ suffer of a
241 species-specific offset (Von Grafenstein et al., 1999; Holmes and Chivas, 2002), to make
242 meaningful comparisons is important to correct the $\delta^{18}\text{O}_{\text{ost}}$ by removing the species-specific
243 offset to normalize the $\delta^{18}\text{O}_{\text{ost}}$ values with the theoretical inorganic calcite deposited at the
244 isotopic equilibrium at the same moment in the same environment. We used the values of these
245 offsets previously calculated and reported for *C. angulata* (2.2‰, Von Grafenstein et al., 1999)
246 and *C. torosa* (0.8‰ Keatings et al., 2007). The vital offset of *S. aculeata* and *H. salina* have
247 never been calculated before and without the analyses of living shells is not possible to validate
248 these values. However, *E. mareotica* is considered to precipitate close to the isotopic
249 equilibrium (Li and Liu, 2010) and because there is no substantial difference between the

250 $\delta^{18}\text{O}_{\text{ost}}$ values of *S. aculeata* and *E. mareotica* (0.009‰ in sample TRAH1-1 and TRAH1-2),
251 we assume that this is also the case for *S. aculeata* and *H. salina* (difference of 0.18 ‰ between
252 TRA2 and TRA2B).

253

254 **3. Results**

255

256 **3.1 Classic and clumped-isotopes**

257

258 The Δ_{47} values of the ostracod samples range from 0.6485 to 0.5941 ‰ with a SE from 0.009
259 to 0.015 ‰ (Table 1). Values of the $\delta^{18}\text{O}_{\text{ost}}$ and $\delta^{13}\text{C}_{\text{ost}}$ vary from -0.45 ‰ to 3.20 ‰ and from
260 -3.47 ‰ to 3.99 ‰ (SE of 0.1 ‰ on average). The number of replicated measurements carried
261 out per sample was determined based on the availability of sample material. The large number
262 of replicates per specimen ensures the robustness of the results. The repeatability along the 8
263 sessions of the standards used to standardize the results and the ostracod samples was 33.2 ppm
264 and 31.4 ppm, respectively. The repeatability of the $\delta^{18}\text{O}_{\text{ost}}$ and $\delta^{13}\text{C}_{\text{ost}}$ was 39.0 ppm and 17.8
265 ppm, respectively. The ETH4 standard, used to assure and control the quality of the analyses,
266 presents a Δ_{47} value of 0.4460 ‰ and a standard error (SE) of 0.0059 for 67 replicates. The
267 difference between our measured value of ETH4 and the official one from Bernasconi et al.,
268 (2021) (ETH2- Δ_{47} value of 0.4505 ± 0.0015) is negligible (Δ_{47} of 0.0045) and falls within the
269 calculated SE. This confirms both the accuracy and precision of the Δ_{47} analyses presented in
270 this study. The box plots for Δ_{47} temperatures (Figure 6) are made including all replicate
271 measurements per each sample (see Table 1 in supplementary material) and show median
272 temperatures of 17 °C during the MIS3, of 12 °C during MIS2 and of 23 °C during the Holocene.
273 The larger probability density in MIS3 and the Holocene is due to the internal higher replicate
274 variability in the measured samples. This differs from the analytical uncertainties reported for

275 each Δ_{47} -temperature data that is, instead, determined using the "pooled" standardization
276 method outlined by Daëron (2021) that considers the reproducibility constraints obtained from
277 both standard and sample analyses.

278

279 **4. Discussion**

280

281 **4.1 Species-specific effect on the ostracod- Δ_{47} paleothermometer**

282

283 In the first application of the ostracod- Δ_{47} thermometer on living ostracod that precipitated their
284 shells at known temperatures, Marchegiano et al. (in review) demonstrated the absence of a
285 vital offset at genus and species level. In this study, to confirm the absence of a species-specific
286 effect also in the fossil record, we analyzed the Δ_{47} of two different ostracod species coming
287 from the same sediment layers that, thus, precipitated their shells at the same time, season and
288 in the same temperature and environment. The absence of a consistent offset, within the
289 analytical uncertainty, between *S. aculeata* (TRA-2) and *H. salina* (TRA2b) (Δ_{47} $0.002 \pm$
290 0.01% , Tab.1) and between *S. aculeata* (TRAH2-1) and *E. mareotica* (TRAH2-2) (Δ_{47} 0.0007
291 $\pm 0.01\%$ Tab.1) confirms the absence of the vital offset in fossil ostracod shells at genus and
292 species level. This finding provides a further confirmation that the ostracod- Δ_{47} thermometer
293 can be applied independently to the ostracod species and throughout the geological time.

294 Although there is no vital offset in the ostracod- Δ_{47} signal, it is important to know the timing
295 of precipitation of ostracod shells to provide accurate paleotemperature reconstructions. As a
296 consequence, not all species can be combined together but only the ones that precipitate their
297 shells during the same season. Thus, by combining the Δ_{47} technique, with paleontological and
298 biological knowledge of the ostracod fauna, the ostracod- Δ_{47} paleothermometer has the
299 potential to reconstruct past temperatures and seasonality variations.

300

301 **4.2 Ostracod- Δ_{47} temperature reconstruction**

302

303 To correctly use ostracod shells as a geochemical tool, it is necessary to understand their
304 ecological preferences and life history (i.e., timing of shell precipitation). The species used in
305 this study are widespread and quite well known.

306 *Cyprideis torosa* (Fig. 4) is a species that can live at a wide range of salinities (Griffith and
307 Holmes, 2000) in permanent water conditions (Meisch, 2000) and was found living today in
308 the freshwater Lake Trasimeno (Marchegiano et al., 2017). This species seems to produce two
309 generations per year with adulthood calcification in spring and autumn (Heip, 1976 and Roberts
310 et al., 2020). Today, the water temperature of Lake Trasimeno ranges from 11 °C (April) to 23
311 °C (June) during spring and from 16 °C (October) to 8 °C (December) in autumn (World Lake
312 database 2023). Δ_{47} analyses made on recent *C. torosa* shells (TRAR2) yield temperatures of
313 22.5 ± 2.3 °C. It therefore seems that, at Lake Trasimeno there is a prevalence of spring
314 generations or that shells continue to calcify also during the summer. In this study, we consider
315 this species as indicative of late-spring/early-autumn (warm season) temperatures (today May-
316 October water mean T are 21.4°C). In the Trasimeno record, *C. torosa* is very abundant during
317 the relatively warm and humid MIS 3 (from ca. 46 to 34 cal ky BP), and the Holocene,
318 indicating a permanent lake with low saline water (Marchegiano et al., 2018 and 2019). The *C.*
319 *torosa* Δ_{47} temperature during MIS 3 ranges from 15 ± 1.6 °C to 22 ± 2.3 °C and of 23.2 ± 2.5
320 °C in the Early Holocene (Table 2).

321 *Sarocypridopsis aculeata* and *Eucypris mareotica* (Fig. 4) are often found together and indicate
322 ephemeral-shallow lake conditions and high salinity conditions (Martin-Puertas et al., 2008).
323 They do not live in Lake Trasimeno today (Marchegiano et al., 2017) and disappeared from
324 the fossil record at the Pleistocene-Holocene transition suggesting a change from prevalent

325 ephemeral to permanent lake conditions (Marchegiano et al., 2018 and 2019). *S. aculeata*
326 develops up to three summer generations per year (time of shells calcification) and adults very
327 rarely survive in the colder months (Meish, 2000). *E. mareotica* hatches between late June and
328 early July and reaches the adults stage in late July-early August (Li and Liu, 2010). Today, the
329 water temperature of Lake Trasimeno during summer ranges from 26°C (August) to 21°C
330 (September) (World Lake database 2023) (Table 2). Δ_{47} analyses on recent *S. aculeata* and *E.*
331 *mareotica*, to confirm their precipitation season in Lake Trasimeno, are not possible because
332 these species are not part of the living fauna today. However, if we assume that during the
333 entire Holocene temperatures were similar to today, the Δ_{47} analyses made on Early Holocene
334 *S. aculeata* shells (TRA2, temperature of $24.9 \pm 2^\circ\text{C}$), could confirm that *S. aculeata*
335 precipitates its shell during the summer season at Lake Trasimeno (today mean water T are of
336 24°C). The seasonal attribution can also be extended to *E. mareotica* since no significant
337 difference in temperature is observed between samples TRAH2-1 (*S. aculeata*) and TRAH2-2
338 (*E. mareotica*) (13 and $13.2 \pm 3^\circ\text{C}$ respectively) that come from the same sediment layers. In
339 the Trasimeno record, *S. aculeata* and *E. mareotica* are the most abundant species at the end
340 of the MIS 3 and during the cold and dry MIS 2 (from ca. 34'000 to 10'300) indicating shallow-
341 ephemeral lake conditions and higher salinities (Marchegiano et al., 2018). The Δ_{47}
342 temperatures derived from *S. aculeata* shells during MIS2 range from $10 \pm 2.9^\circ\text{C}$ to 17 ± 3.1
343 $^\circ\text{C}$ and it is of $24.9 \pm 2^\circ\text{C}$ at the Pleistocene-Holocene transition (Table 2).

344 *Heterocypris salina* (Fig. 4) is a cosmopolitan species often found together with *S. aculeata*
345 and *C. torosa* but it does not tolerate ephemeral conditions. This species lives today in Lake
346 Trasimeno (Marchegiano et al., 2017). It has 2 to 3 summer generations (time of shells
347 calcification) and lives for 45 days (Meish, 2000). At the Pleistocene-Holocene transition,
348 samples TRA 2 and TRA 2B, *S. aculeata* and *H. salina* were measured and provided a very

349 close temperature (24.9 ± 2 °C and 24.3 ± 2.2 °C respectively) confirming that they both
350 precipitate during the summer season (Fig. 5 and Table 2).

351 *Candona angulata* (Fig. 4) prefers slightly salty permanent waters and it is often found together
352 with *H. salina* and *C. torosa*. This species today lives in the deepest part of Lake Trasimeno in
353 association with *C. torosa* (Marchegiano et al., 2017). *C. angulata* is a winter species that lives
354 from November to March and precipitates its shell from November to February (Meish, 2000).
355 Today, the winter water temperatures at Lake Trasimeno range from 12°C (November) to 7°C
356 (February) (World Lake database 2023). In the Trasimeno record, *C. angulata* is present almost
357 during the entire interval, but it is found at such small percentages that Δ_{47} analyses could not
358 be conducted. It is, instead, very abundant in the Holocene and in this study was used to
359 reconstruct seasonal variations during this time period. The Δ_{47} analyses made on *C. angulata*
360 (TRAR2) gave temperatures of 8 ± 2.9 °C in recent shells and of 11.8 ± 2.1 °C in the Early
361 Holocene (TRAHOL1) (Fig. 5 and Table 2). On the same samples *C. torosa*, a late-
362 spring/early-autumn species, recorded temperatures of 22.5 ± 2.3 °C and 23.2 ± 2.5 °C
363 respectively (Fig. 5). The good correspondence with the today mean water temperatures of
364 Lake Trasimeno (8°C during November-February and of 21.4°C during May-October)
365 confirms the accuracy of the analyses, the applicability of the ostracod- Δ_{47} on fossil shells and
366 its ability in reconstruct paleotemperatures, even at seasonal scale.

367

368 **4.3. Paleoclimate reconstruction**

369

370 In this study, all Δ_{47} temperatures measured on *C. torosa*, *S. aculeata*, *E. mareotica*, and *H.*
371 *salina* shells are considered as warm season temperature (from late spring to early autumn).
372 Instead, Δ_{47} temperatures from *C. angulata* are considered as cold season temperatures (from
373 November to March).

374 Warm season water temperatures based on ostracod- Δ_{47} fall into the July minimum and
375 maximum mutual ostracod air temperature range (MOTR) reconstructed for this interval by
376 Marchegiano et al. (2020), within the uncertainties, and correspond well to the peak (higher T)
377 and minima (lower T) of the MOTR curves (Fig. 5). This suggests a close connection between
378 air and water temperature variations in Lake Trasimeno and a prompt reaction of the lake
379 system to climatic changes. The LATEMIS3 (Table 1) is the only sample, including the Δ_{47}
380 uncertainties, that falls outside the MOTR (Fig. 5). This could be explained by a lack of (or
381 reduced) response of the ostracod fauna (i.e., change in the ostracod assemblages) to the fast
382 environmental change at the onset of this cold event (probably associated to H3).

383 Colder and warmer periods at Lake Trasimeno are certainly linked to the millennial-scale
384 climatic variations (warm-humid interstadial GI, cold-arid stadial GS and coldest and driest
385 Heinrich events), as confirmed by prior studies (Marchegiano et al., 2018, 2020 and Francke
386 et al., 2022). These millennial-scale climatic events are likely associated to reduction (cold
387 events) and enhancing (warm events) of the Atlantic Meridional Overturning Circulation
388 (AMOC) plus a displacement of cooling conditions throughout the central Mediterranean area
389 during the GS and Heinrich events (Francke et al., 2022). However, because of chronological
390 limitations, it is not possible to identify exactly which events have been recorded.

391 The *C. torosa*- Δ_{47} temperatures during MIS3 ranges from 15 ± 1.6 °C to 22 ± 2.3 °C, with a
392 median temperature of 17 °C, indicating that warm season temperatures were from 2 to 6 °C
393 lower than today (Fig. 6 and Table 2). During the same interval, air temperatures of the coldest
394 month based on pollen from south Italy (Lake Monticchio) are around -8°C, reaching -16 °C
395 in the coldest events (Allen et al., 1999). Meanwhile, marine annual surface temperatures based
396 on alkenones for the Alboran Sea range from 10 to 16°C (Cacho et al., 1999) (Fig. 6). In this
397 interval, the coldest event (15 ± 1.6 °C) at Lake Trasimeno could be tentatively associated to
398 the Heinrich events (H4). Likewise, the warmest events (20 ± 2.1 and 22 ± 2.3 °C) are likely

399 linked to the GIs (10 and 8) and the event at ca. 18 ± 1.7 °C to is probably associated with the
400 GS (12).

401 At the transition between MIS 3 and MIS 2, which corresponds to the onset of full glacial
402 conditions, *S. aculeata*- Δ_{47} warm season temperature drastically decrease to 10 ± 2.9 °C and
403 then slowly increase up to 15 ± 3 °C at the end of MIS 2. The median warm season temperature
404 for the MIS2 is 12°C (from 12 to 7 °C colder than today warm season mean temperatures) (Fig.
405 6). The substantial decrease in temperature observed at Lake Trasimeno is only marginally
406 reflected in the marine surface mean annual temperatures at the Alboran Sea and it is nearly
407 absent in the Monticchio winter temperature, which remains around -8°C. This divergence in
408 behavior, between the three records may be attributed to a diverse climate response and/or the
409 influence of regional parameters. However, differences between the air temperature of the
410 coldest month (pollen from Lake Monticchio, southern Italy) and warm season water
411 temperatures (Δ_{47} – ostracod from Lake Trasimeno, central Italy) can potentially be explained
412 by the reduced summer insolation experienced during MIS2 (Fig. 6). The coldest temperatures
413 in this interval could be tentatively associated to the Heinrich's events. If we consider that the
414 last cold event of this interval was the Younger Dryas, summer temperatures at Lake Trasimeno
415 (15 ± 3 °C) are very comparable to the pollen summer temperature at Lake Matese (southern
416 Italy, Robles et al., 2023) and the chironomid summer temperatures at Lake Piccolo di
417 Avigliana (northern Italy, Larocque and Finsinger, 2008) both recording a temperature of 16
418 °C. The brGDGT mean annual temperatures of Lake Matese, in the same period, is instead 12
419 °C (Robles et al., 2023) (Fig. 6).

420 At the Pleistocene - Holocene transition (i.e., the onset of the interglacial), warmer season
421 temperatures increased in 10 °C (temperatures of 25 ± 2 °C, 3 °C higher than the warmer season
422 temperatures today, see Table 2) with Holocene median temperatures of 23°C (Fig. 6). Because
423 of the very shallow/ephemeral conditions of Lake Trasimeno during MIS 2 and the Pleistocene

424 – Holocene transition (Marchegiano et al., 2018 and 2019), a possible overestimation of lake
425 water temperatures from 2 to 4 °C (i.e., the modern temperature difference between lake water
426 and atmosphere at Lake Trasimeno today) need to be considered as temperatures could be
427 closer to the atmospheric ones.

428 During the Early Holocene, the warm season temperatures closely resemble those of the present
429 day. However, the cold season temperature (12 ± 2.1 °C) is approximately 4°C warmer than
430 those of today (8°C), indicating a reduced seasonality (Fig. 6). This decrease in seasonality
431 during the Early Holocene aligns well with previous findings in hydrological records from
432 central-southern Italy (Magny et al., 2012 and Marchegiano et al., 2019). The temperature
433 record based on Δ_{47} measurements from Lake Trasimeno provides the first confirmation of a
434 lower seasonality, also in temperatures, than today for central-southern Italy.

435 Latest Holocene (last ca. 1 ky) Δ_{47} temperatures are the same as today at Lake Trasimeno (8°C
436 winter and 22°C for late spring/early autumn).

437

438 **4.4 Paleohydrology reconstruction**

439

440 Because of the endoreic and shallow nature of Lake Trasimeno, its water geochemistry is
441 strictly dependent on the climatic variations and particularly, on the E/P (Froncini et al., 2019;
442 Ludovisi and Gaino, 2010). This was confirmed by the comparison between recent $\delta^{18}\text{O}$ and
443 $\delta^2\text{H}$ lake water values and the local evaporation line (LEL) (Froncini et al., 2019) and by the
444 moderate positive correlation ($R^2= 0.24$) between past $\delta^{13}\text{C}$ and $\delta^{18}\text{O}$ in bulk carbonates data
445 indicating an exchange between lake water and atmosphere due to evaporation (Francke et al.,
446 2022). The oxygen isotopic composition of precipitation ($\delta^{18}\text{O}_p$) at Lake Trasimeno today
447 varies between -9.9‰ in January and -1.9‰ in July (Waterisotopes Database, 2017) as a
448 consequence of decreasing summer precipitation and increasing temperatures. The differences

449 between $\delta^{18}\text{O}_p$ and $\delta^{18}\text{O}_w$ today is between ca. 9 and 11 ‰ during winter and ca. 3 and 6 ‰
450 during summer, indicating a large loss of light isotope ($\delta^{16}\text{O}$) through evaporation. However,
451 the small difference of 2 ‰ between today $\delta^{18}\text{O}_w$ summer (ca. 3.8 to 1.2 ‰) and $\delta^{18}\text{O}_w$ winter
452 (-1 to 1 ‰) (monitored values from Frondini et al., 2019) also suggests a minor contribution
453 of summer precipitation to the annual $\delta^{18}\text{O}_w$ budget.

454 There is a good agreement between the $\delta^{18}\text{O}_w$ values reconstructed from ostracod shells and
455 the $\delta^{18}\text{O}$ curve on bulk carbonate from Francke et al., (2022) suggesting a co-variance of these
456 two isotopic signals (Fig. 5). However, the slight difference in the absolute values between
457 $\delta^{18}\text{O}$ of calcite (measured on bulk carbonate) and $\delta^{18}\text{O}_w$ of the water (measured on ostracods)
458 could be due to both the isotopic fractionation between $\delta^{18}\text{O}$ of the water and the one recorded
459 in the carbonate as well as a difference in timing of carbonate precipitation between ostracod
460 (few hours and related to the calcification season) and bulk carbonate (annual average).

461 During the mild and more humid MIS 3, $\delta^{18}\text{O}_w$ warm season values range from 2.0 ± 0.2 to 1.0
462 ± 0.2 ‰, within the range of present-day variability. Lower values correspond to colder
463 temperatures (18 ± 1.7 °C) and higher values to warmer ones (ca. 22 ± 2.3 °C) suggesting
464 colder-drier and warmer-humid periods. Although ostracod assemblages indicate permanent
465 lake conditions, they also suggest that the variations in precipitation and/or evaporation amount
466 are very low.

467 During the cold and arid MIS2, $\delta^{18}\text{O}_w$ warm season values range from 1.5 ± 0.3 to 0 ± 0.3 ‰
468 (Fig. 5). Considering that several studies suggest a decrease in precipitation during MIS2 in the
469 central Mediterranean area (e.g., Allen et al., 1999; Follieri et al., 1988), and that ostracod
470 assemblages at Lake Trasimeno also indicate low lake level/ephemeral conditions
471 (Marchegiano et al., 2018), the lighter values during MIS2 compared to MIS3 could be due to
472 a decrease of evaporation as consequence of lower summer insolation (Figure 5).

473 At the Pleistocene – Holocene transition, $\delta^{18}\text{O}_w$ warmer season values are the highest of the
474 entire interval ($\delta^{18}\text{O}_w 2.7 \pm 0.2 \text{ ‰}$) probably due to an increase in evaporation (water enriched
475 of heavier $\delta^{18}\text{O}$) caused by high temperatures and highest summer insolation (Figure 5).
476 Ostracod assemblages still indicate low lake level/ephemeral conditions (Marchegiano et al.,
477 2018) suggesting conditions more arid than today, as also recorded by pollen archives from
478 southern and central Italy (Magny et al., 2012).

479 In the Early Holocene, $\delta^{18}\text{O}_w$ decrease and warm and cold season values are very close ($\delta^{18}\text{O}_w$
480 1 ± 0.2 and $0.9 \pm 0.2 \text{ ‰}$) (Figure 5). Ostracod assemblages indicate an increase of lake level
481 (Marchegiano et al., 2019), these values suggest lower E/P ratios (and thus high humidity)
482 during both seasons, indicating a low seasonality contrast in the hydrology. However, seasonal
483 temperatures are instead very different (11.8 ± 2.1 and $23.2 \pm 2.5 \text{ °C}$). The same
484 paleohydrological behavior has been observed in Lake Pergusa and Lake Preola (southern
485 Italy) (Magny et al., 2012) as well as in eastern Mediterranean (Kolodny et al., 2005; Marino
486 et al., 2009; Develle et al., 2010). Conversely, records from northern Italy and western
487 Mediterranean recorded a higher seasonality contrast with drier summers during and after ca.
488 9800 cal a BP (Finsinger et al., 2010 and Peyron et al., 2011). This study also confirms that,
489 during the Early Holocene, climatic conditions in central Italy were similar to those ones in
490 southern Italy and, thus, that the climatic limit between northern and southern climatic zone in
491 Italy, previously settled at 40° latitude by Magny et al. (2012), needs to be moved to 43°
492 latitude, as previously suggested by Marchegiano et al. (2019).

493 In the latest part of the Holocene, the reconstructed $\delta^{18}\text{O}_w$ values (Fig. 5) are very similar to
494 today ones and indicate a difference of 2 ‰ between seasons suggesting high winter and low
495 summer precipitation as typical of present-day central Mediterranean climate. This larger
496 contrast of precipitation amount between seasons seems to have started in central – southern
497 Italy around ca. 4.5 cal ky BP (Magny et al., 2012). Similar seasonal patterns in precipitations

498 have been also observed in the western Mediterranean (García-Alix et al., 2021; Toney et al.,
499 2020)

500

501 **5. CONCLUSIONS**

502

503 - The analyses made on recent samples (last ca. 1ky) confirm the applicability of the
504 ostracod-clumped isotope thermometer to reconstruct paleotemperatures, seasonality
505 and hydrological conditions.

506 - The absence of a vital effect at genus and species level is confirmed also in the signal
507 of fossil Δ_{47} -ostracod shells signal.

508 - Despite the absence of a vital effect, in environments with seasonal temperature
509 variations, not all species can be combined and measured together, instead only those
510 that precipitate their shell during the same season.

511 - The MOTR technique is a very useful high-resolution proxy for identifying the larger
512 temperature variations to select the samples for further Δ_{47} analyses.

513 - The application of the ostracod- Δ_{47} thermometer on the Trasimeno lacustrine core
514 (central Italy), provides the first continental warm season paleotemperature and
515 hydrological conditions for the last 43 ky in the central Mediterranean area.

516 - Warm season temperatures were heavily impacted by millennial scale climatic events.

517 - Insolation conditions in the central Mediterranean area enhanced the effect of the
518 millennial scale climate variability, by increasing warm season temperature differences
519 between warmer/high insolation MIS 3 (median temperatures of 17 °C) and
520 colder/lower insolation MIS2 (median temperatures of 12 °C). This trend is also
521 observed in warm season hydrological conditions with high evaporation during MIS3
522 and low ones in the MIS2.

523 - During the Early Holocene warmer than today cold season temperatures are observed
524 and similar hydrological conditions between warm and cold season underlying a lower
525 seasonality contrast than today and enhanced warm season precipitation.

526

527 **DECLARATION OF COMPETING INTEREST**

528 The authors declare that they have no known competing financial interests or personal
529 relationships that could have appeared to influence the work reported in this paper.

530

531 **ACKNOWLEDGMENTS**

532 We thank the AMGC-VUB technician David Verstraeten for his immensurable help and
533 support during the analyses. David De Vleeschower and Jose Manuel Mesa-Fernández for the
534 very helpful discussions. The study was in part funded by Junta de Andalucía-Consejería de
535 Universidad, Investigación e Innovación-Proyecto 21.00020. MM wish to express their thanks
536 for the financial support of the Swiss National Science Foundation (P2GEP2_181063). PC,
537 SG. and CS thank the Research Foundation Flanders for funding the IRMS acquisition and the
538 VUB Strategic Research for support.

539

540 **DATA AVAILABILITY**

541 Data are available in the supplementary material section during the review process, and they
542 will be successively deposited in a data repository, most probably EarthChem.

543

544 **REFERENCES**

545

546 Abrantes, F., Voelker, A. (Helga L., Sierro, F.J., Naughton, F., Rodrigues, T., Cacho, I.,
547 Ariztegui, D., Brayshaw, D., Sicre, M.-A., Batista, L., 2012. Paleoclimate Variability in

548 the Mediterranean Region, in: *The Climate of the Mediterranean Region*. Elsevier, pp.
549 1–86. <https://doi.org/10.1016/B978-0-12-416042-2.00001-X>

550 Ali, E., W. Cramer, J. Carnicer, E. Georgopoulou, N.J.M. Hilmi, G. Le Cozannet, and P.
551 Lionello, 2022: Cross-Chapter Paper 4: Mediterranean Region. In: *Climate Change*
552 *2022: Impacts, Adaptation, and Vulnerability*. Contribution of Working Group II to the
553 Sixth Assessment Report of the Intergovernmental Panel on Climate Change [H.-O.
554 Pörtner, D.C. Roberts, M. Tignor, E.S. Poloczanska, K. Mintenbeck, A. Alegría, M.
555 Craig, S. Langsdorf, S. Löschke, V. Möller, A. Okem, B. Rama (eds.)]. Cambridge
556 University Press, Cambridge, UK and New York, NY, USA, pp. 2233-2272,
557 doi:10.1017/9781009325844.021

558

559 Allen, J.R.M., Brandt, U., Brauer, A., Hubberten, H.-W., Huntley, B., Keller, J., Kraml, M.,
560 Mackensen, A., Mingram, J., Negendank, J.F.W., Nowaczyk, N.R., Oberhänsli, H.,
561 Watts, W.A., Wulf, S., Zolitschka, B., 1999. Rapid environmental changes in southern
562 Europe during the last glacial period. *Nature* 400, 740–743.
563 <https://doi.org/10.1038/23432>

564 Anderson, N., Kelson, J.R., Kele, S., Daëron, M., Bonifacie, M., Horita, J., Mackey, T.J., John,
565 C.M., Kluge, T., Petschnig, P., Jost, A.B., Huntington, K.W., Bernasconi, S.M.,
566 Bergmann, K.D., 2021. A unified clumped isotope thermometer calibration (0.5-1100C)
567 using carbonate-based standardization (preprint). *Geochemistry*.
568 <https://doi.org/10.1002/essoar.10505702.1>

569 Bernasconi, S.M., Daëron, M., Bergmann, K.D., Bonifacie, M., Meckler, A.N., Affek, H.P.,
570 Anderson, N., Bajnai, D., Barkan, E., Beverly, E., Blamart, D., Burgener, L., Calmels,
571 D., Chaduteau, C., Clog, M., Davidheiser-Kroll, B., Davies, A., Dux, F., Eiler, J., Elliott,
572 B., Fetrow, A.C., Fiebig, J., Goldberg, S., Hermoso, M., Huntington, K.W., Hyland, E.,
573 Ingalls, M., Jaggi, M., John, C.M., Jost, A.B., Katz, S., Kelson, J., Kluge, T., Kocken,

574 I.J., Laskar, A., Leutert, T.J., Liang, D., Lucarelli, J., Mackey, T.J., Mangenot, X.,
575 Meinicke, N., Modestou, S.E., Müller, I.A., Murray, S., Neary, A., Packard, N., Passey,
576 B.H., Pelletier, E., Petersen, S., Piasecki, A., Schauer, A., Snell, K.E., Swart, P.K.,
577 Tripathi, A., Upadhyay, D., Vennemann, T., Winkelstern, I., Yarian, D., Yoshida, N.,
578 Zhang, N., Ziegler, M., 2021. InterCarb: A Community Effort to Improve Interlaboratory
579 Standardization of the Carbonate Clumped Isotope Thermometer Using Carbonate
580 Standards. *Geochem Geophys Geosyst* 22. <https://doi.org/10.1029/2020GC009588>

581 Blaauw, M., Christen, J.A., 2011. Flexible paleoclimate age-depth models using an
582 autoregressive gamma process. *Bayesian Anal.* 6. <https://doi.org/10.1214/11-BA618>

583 Blaauw, M., Christen, J.A., Bennett, K.D., Reimer, P.J., 2018. Double the dates and go for
584 Bayes — Impacts of model choice, dating density and quality on chronologies.
585 *Quaternary Science Reviews* 188, 58–66.
586 <https://doi.org/10.1016/j.quascirev.2018.03.032>

587 Börner, N., De Baere, B., Yang, Q., Jochum, K.P., Frenzel, P., Andreae, M.O., Schwalb, A.,
588 2013. Ostracod shell chemistry as proxy for paleoenvironmental change. *Quaternary*
589 *International* 313–314, 17–37. <https://doi.org/10.1016/j.quaint.2013.09.041>

590 Cacho, I., Grimalt, J.O., Pelejero, C., Canals, M., Sierro, F.J., Flores, J.A., Shackleton, N.,
591 1999. Dansgaard-Oeschger and Heinrich event imprints in Alboran Sea
592 paleotemperatures. *Paleoceanography* 14, 698–705.
593 <https://doi.org/10.1029/1999PA900044>

594 Chivas, A.R., De Deckker, P., Shelley, J.M.G., 1983. Magnesium, strontium and barium
595 partitioning in non marine ostracod shells and their use in paleoenvironment
596 reconstructions – a preliminary study., in: *Applications of Ostracoda*. University of
597 Houston, TX, pp. 238–249.

598 Cohen, A.S., 2003. Paleolimnology: the history and evolution of lake systems. Oxford
599 University Press, New York.

600 Daëron, M., 2021. Full Propagation of Analytical Uncertainties in Δ_{47} Measurements.
601 *Geochem Geophys Geosyst* 22. <https://doi.org/10.1029/2020GC009592>

602 Daëron, M., Blamart, D., Peral, M., Affek, H.P., 2016. Absolute isotopic abundance ratios and
603 the accuracy of Δ_{47} measurements. *Chemical Geology* 442, 83–96.
604 <https://doi.org/10.1016/j.chemgeo.2016.08.014>

605 Develle AL, Herreros J, Vidal L, et al. 2010. Controlling factors on a palaeo-lake oxygen
606 isotope record (Yammo'neh, Lebanon) since the Last Glacial Maximum. *Quaternary*
607 *Science Reviews* 29: 865886.

608 De Vleeschouwer, D., Peral, M., Marchegiano, M., Füllberg, A., Meinicke, N., Pälike, H.,
609 Auer, G., Petrick, B., Snoeck, C., Goderis, S., Claeys, P., 2022. Plio-Pleistocene Perth
610 Basin water temperatures and Leeuwin Current dynamics (Indian Ocean) derived from
611 oxygen and clumped-isotope paleothermometry. *Clim. Past* 18, 1231–1253.
612 <https://doi.org/10.5194/cp-18-1231-2022>

613 de Winter, N.J., Müller, I.A., Kocken, I.J., Thibault, N., Ullmann, C.V., Farnsworth, A., Lunt,
614 D.J., Claeys, P., Ziegler, M., 2021. Absolute seasonal temperature estimates from
615 clumped isotopes in bivalve shells suggest warm and variable greenhouse climate.
616 *Commun Earth Environ* 2, 121. <https://doi.org/10.1038/s43247-021-00193-9>

617 Eiler, J.M., 2007. “Clumped-isotope” geochemistry—The study of naturally-occurring,
618 multiply-substituted isotopologues. *Earth and Planetary Science Letters* 262, 309–327.
619 <https://doi.org/10.1016/j.epsl.2007.08.020>

620 Finsinger W, Colombaroli D, de Beaulieu JL, et al. 2010. Early to midHolocene climate change
621 at Lago dell'Accesa (central Italy): climate signal or anthropogenic bias? *Journal of*
622 *Quaternary Science* 25: 1239–1247.

623 Follieri, M., Magri, D., Sadori, L., 1988. 250'000-year pollen record from Valle di Castiglione
624 (Roma). *Pollen et Spore* 33, 329–356.

625 Francke, A., Lacey, J.H., Marchegiano, M., Wagner, B., Ariztegui, D., Zanchetta, G., Kusch,
626 S., Ufer, K., Baneschi, I., Knödgen, K., 2021. Last Glacial central Mediterranean
627 hydrology inferred from Lake Trasimeno's (Italy) calcium carbonate geochemistry.
628 *Boreas* bor.12552. <https://doi.org/10.1111/bor.12552>

629 Frondini, Dragoni, Morgantini, Donnini, Cardellini, Caliro, Melillo, Chiodini, 2019. An
630 Endorheic Lake in a Changing Climate: Geochemical Investigations at Lake Trasimeno
631 (Italy). *Water* 11, 1319. <https://doi.org/10.3390/w11071319>

632 García-Alix, A., Camuera, J., Ramos-Román, M.J., Toney, J.L., Sachse, D., Schefuß, E.,
633 Jiménez-Moreno, G., Jiménez-Espejo, F.J., López-Avilés, A., Anderson, R.S., Yanes, Y.,
634 2021. Paleohydrological dynamics in the Western Mediterranean during the last glacial
635 cycle. *Global and Planetary Change* 202, 103527.
636 <https://doi.org/10.1016/j.gloplacha.2021.103527>

637 Gasperini, L., Barchi, M.R., Bellucci, L.G., Bortoluzzi, G., Ligi, M., Pauselli, C., 2010.
638 Tectonostratigraphy of Lake Trasimeno (Italy) and the geological evolution of the
639 Northern Apennines. *Tectonophysics* 492, 164–174.
640 <https://doi.org/10.1016/j.tecto.2010.06.010>

641 Gasperini, L., Peteet, D., Bonatti, E., Gambini, E., Polonia, A., Nichols, J., Heusser, L., 2022.
642 Late Glacial and Holocene environmental variability, Lago Trasimeno, Italy. *Quaternary*
643 *International* 622, 21–35. <https://doi.org/10.1016/j.quaint.2021.10.011>

644 Gornitz, V. (Ed.), 2009. *Encyclopedia of paleoclimatology and ancient environments*,
645 *Encyclopedia of earth sciences series*. Springer, Dordrecht, Netherlands ; New York.

646 Grafenstein, U. von, Erlenkeuser, H., Brauer, A., Jouzel, J., Johnsen, S.J., 1999. A Mid-
647 European Decadal Isotope-Climature Record from 15,500 to 5000 Years B.P. *Science* 284,
648 1654–1657. <https://doi.org/10.1126/science.284.5420.1654>

649 Griffiths, H.I. and Holmes, J.A., 2000. Non-marine ostracods and Quaternary
650 palaeoenvironments. *Quaternary Research Association Technical Guide* 8, 179.

651 Heiri, O., Ilyashuk, B., Millet, L., Samartin, S., Lotter, A.F., 2015. Stacking of discontinuous
652 regional palaeoclimate records: Chironomid-based summer temperatures from the
653 Alpine region. *The Holocene* 25, 137–149. <https://doi.org/10.1177/0959683614556382>

654 Heip, C., 1976, The life-cycle of *Cyprideis torosa* (Crustacea, Ostracoda): *Oecologia*, v. 24,
655 p. 229–245.

656 Henkes, G.A., Passey, B.H., Wanamaker, A.D., Grossman, E.L., Ambrose, W.G., Carroll,
657 M.L., 2013. Carbonate clumped isotope compositions of modern marine mollusk and
658 brachiopod shells. *Geochimica et Cosmochimica Acta* 106, 307–325.
659 <https://doi.org/10.1016/j.gca.2012.12.020>

660 Holmes, J.A., Chivas, A.R., 2002. Ostracod shell chemistry — overview, in: Holmes, J.A.,
661 Chivas, A.R. (Eds.), *Geophysical Monograph Series*. American Geophysical Union,
662 Washington, D. C., pp. 185–204. <https://doi.org/10.1029/131GM10>

663 Holmes, J.A., De Deckker, P., 2012. The Chemical Composition of Ostracod Shells, in:
664 *Developments in Quaternary Sciences*. Elsevier, pp. 131–143.
665 <https://doi.org/10.1016/B978-0-444-53636-5.00008-1>

666 Horne, D.J., 2007. A Mutual Temperature Range method for Quaternary palaeoclimatic
667 analysis using European nonmarine Ostracoda. *Quaternary Science Reviews* 26, 1398–
668 1415. <https://doi.org/10.1016/j.quascirev.2007.03.006>

669 John, C.M., Bowen, D., 2016. Community software for challenging isotope analysis: First
670 applications of ‘Easotope’ to clumped isotopes: Community software for challenging

671 isotope analysis. *Rapid Commun. Mass Spectrom.* 30, 2285–2300.
672 <https://doi.org/10.1002/rcm.7720>

673 Keatings, K.W., Hawkes, I., Holmes, J.A., Flower, R.J., Leng, M.J., Abu-Zied, R.H., Lord,
674 A.R., 2007. Evaluation of ostracod-based palaeoenvironmental reconstruction with
675 instrumental data from the arid Faiyum Depression, Egypt. *J Paleolimnol* 38, 261–283.
676 <https://doi.org/10.1007/s10933-006-9074-x>

677 Kim, S.T., O’Neil, J.R., 1997. Equilibrium and nonequilibrium oxygen isotope effects in
678 synthetic carbonates. *Geochimica et Cosmochimica Acta* 61, 3461–3475.
679 [https://doi.org/10.1016/S0016-7037\(97\)00169-5](https://doi.org/10.1016/S0016-7037(97)00169-5)

680 Kolodny Y, Stein M, Machlus M. 2005. Sea-rain-lake relation in the Last Glacial East
681 Mediterranean revealed by d18O–d13C in Lake Lisan aragonites. *Geochimica et*
682 *Cosmochimica. Acta* 69: 4045–4060

683 Larocque, I., Finsinger, W., 2008. Late-glacial chironomid-based temperature reconstructions
684 for Lago Piccolo di Avigliana in the southwestern Alps (Italy). *Palaeogeography,*
685 *Palaeoclimatology, Palaeoecology* 257, 207–223.
686 <https://doi.org/10.1016/j.palaeo.2007.10.021>

687 Laskar, J., Robutel, P., Joutel, F., Gastineau, M., Correia, A.C.M., Levrard, B., 2004. A long-
688 term numerical solution for the insolation quantities of the Earth. *A&A* 428, 261–285.
689 <https://doi.org/10.1051/0004-6361:20041335>

690 Li, X., Liu, W., 2010. Oxygen isotope fractionation in the ostracod *Eucypris mareotica*: results
691 from a culture experiment and implications for paleoclimate reconstruction. *J*
692 *Paleolimnol* 43, 111–120. <https://doi.org/10.1007/s10933-009-9317-8>

693 Lionello, P., Scarascia, L., 2018. The relation between climate change in the Mediterranean
694 region and global warming. *Reg Environ Change* 18, 1481–1493.
695 <https://doi.org/10.1007/s10113-018-1290-1>

696 Ludovisi, A., Gaino, E., 2010. Meteorological and water quality changes in Lake Trasimeno
697 (Umbria, Italy) during the last fifty years. *J Limnol* 69, 174.
698 <https://doi.org/10.4081/jlimnol.2010.174>

699 Magny, M., Peyron, O., Sadori, L., Ortu, E., Zanchetta, G., Vanniere, B., Tinner, W., 2012
700 Contrasting patterns of precipitation seasonality during the Holocene in the south- and
701 north-Central Mediterranean *Journal of Quaternary Science*, 27, 290-296

702 Marchegiano M., Peral M., Venderickx J., Martens K., García-Alix A., Snoeck, C. Goderis
703 S., and Claeys P. The ostracod clumped-isotope thermometer: A novel tool to
704 reconstruct quantitative continental climate changes. under review in *Geology*.

705 Marchegiano, M., Gliozzi, E., Ceschin, S., Mazzini, I., Adatte, T., Mazza, R., Ariztegui, D.,
706 2017. Ecology and distribution of living ostracod assemblages in a shallow endorheic
707 lake: the example of the Lake Trasimeno (Umbria, central Italy). *J Limnol*.
708 <https://doi.org/10.4081/jlimnol.2017.1478>

709 Marchegiano, M., Francke, A., Gliozzi, E., Ariztegui, D., 2018. Arid and humid phases in
710 central Italy during the Late Pleistocene revealed by the Lake Trasimeno ostracod record.
711 *Palaeogeography, Palaeoclimatology, Palaeoecology* 490, 55–69.
712 <https://doi.org/10.1016/j.palaeo.2017.09.033>

713 Marchegiano, M., Francke, A., Gliozzi, E., Wagner, B., Ariztegui, D., 2019. High-resolution
714 palaeohydrological reconstruction of central Italy during the Holocene. *The Holocene*
715 29, 481–492. <https://doi.org/10.1177/0959683618816465>

716 Marchegiano, M., Horne, D.J., Gliozzi, E., Francke, A., Wagner, B., Ariztegui, D., 2020. Rapid
717 Late Pleistocene climate change reconstructed from a lacustrine ostracod record in
718 central Italy (Lake Trasimeno, Umbria). *Boreas* 49, 739–750.
719 <https://doi.org/10.1111/bor.12450>

720 Marchegiano, M., John, C.M., 2022. Disentangling the Impact of Global and Regional Climate
721 Changes During the Middle Eocene in the Hampshire Basin: New Insights From
722 Carbonate Clumped Isotopes and Ostracod Assemblages. *Paleoceanog and Paleoclimatol*
723 37. <https://doi.org/10.1029/2021PA004299>

724 Marino G, Rohling EJ, Sangiorgi F, et al. 2009. Early and middle Holocene in the Aegean Sea:
725 interplay between high and low latitude climate variability. *Quaternary Science Reviews*
726 28: 3246–3262

727 Martin-Puertas, C., Valero-Garces, B.L., Pilar Mata, M., Gonzalez-Samperiz, P., Bao, R.,
728 Moreno, A., Stefanova, V., 2008. Arid and humid phases in southern Spain during the
729 last 4000 years: the Zonar Lake record, Cordoba. *The Holocene* 18, 907–921. [http://](http://dx.doi.org/10.1177/0959683608093533)
730 dx.doi.org/10.1177/0959683608093533.

731 Meinicke, N., Reimi, M.A., Ravelo, A.C., Meckler, A.N., 2021. Coupled Mg/Ca and Clumped
732 Isotope Measurements Indicate Lack of Substantial Mixed Layer Cooling in the Western
733 Pacific Warm Pool During the Last ~5 Million Years. *Paleoceanogr Paleoclimatol* 36.
734 <https://doi.org/10.1029/2020PA004115>

735 Meisch, C. (Ed.), 2000. *Ostracoda, Süßwasserfauna von Mitteleuropa / begr. von A. Brauer.*
736 Hrsg. von J. Schwoerbel. Spektrum Akad. Verl, Heidelberg Berlin.

737 Mischke, S., Aichner, B., Diekmann, B., Herzsuh, U., Plessen, B., Wünnemann, B., Zhang,
738 C., 2010. Ostracods and stable isotopes of a late glacial and Holocene lake record from
739 the NE Tibetan Plateau. *Chemical Geology* 276, 95–103.
740 <https://doi.org/10.1016/j.chemgeo.2010.06.003>

741 Pallottini, M., Pagliarini, S., Catasti, M., La Porta, G., Selvaggi, R., Gaino, E., Spacone, L., Di
742 Giulio, A.M., Ali, A., Goretti, E., 2023. Population Dynamics and Seasonal Patterns of
743 *Chironomus plumosus* (Diptera, Chironomidae) in the Shallow Lake Trasimeno, Central
744 Italy. *Sustainability* 15, 851. <https://doi.org/10.3390/su15010851>

745 Peyron O, Goring S, Dormoy I, et al. 2011. Holocene seasonality changes in the central
746 Mediterranean region reconstructed from the pollen sequences of Lake Accesa (Italy)
747 and Tenaghi Philippon (Greece). *The Holocene* 21: 131–147.

748 Peral, M., Blamart, D., Bassinot, F., Daëron, M., Dewilde, F., Rebaubier, H., Nomade, S.,
749 Girone, A., Marino, M., Maiorano, P., Ciaranfi, N., 2020. Changes in temperature and
750 oxygen isotopic composition of Mediterranean water during the Mid-Pleistocene
751 transition in the Montalbano Jonico section (southern Italy) using the clumped-isotope
752 thermometer. *Palaeogeography, Palaeoclimatology, Palaeoecology* 544, 109603.
753 <https://doi.org/10.1016/j.palaeo.2020.109603>

754 Pérez, L., Frenzel, P., Brenner, M., Escobar, J., Hoelzmann, P., Scharf, B., Schwalb, A., 2011.
755 Late Quaternary (24–10 ka BP) environmental history of the Neotropical lowlands
756 inferred from ostracodes in sediments of Lago Petén Itzá, Guatemala. *J Paleolimnol* 46,
757 59–74. <https://doi.org/10.1007/s10933-011-9514-0>

758 Rasmussen, T.L., Thomsen, E., Moros, M., 2016. North Atlantic warming during Dansgaard-
759 Oeschger events synchronous with Antarctic warming and out-of-phase with Greenland
760 climate. *Sci Rep* 6, 20535. <https://doi.org/10.1038/srep20535>

761 Reimer, P.J., 2020. Composition and consequences of the IntCal20 radiocarbon calibration
762 curve. *Quat. res.* 96, 22–27. <https://doi.org/10.1017/qua.2020.42>

763 Roberts, L.R., Holmes, J.A., Horne, D.J., 2020. Tracking the seasonal calcification of *Cyprideis*
764 *torosa* (Crustacea, Ostracoda) using Mg/Ca-inferred temperatures, and its implications
765 for palaeotemperature reconstruction. *Marine Micropaleontology* 156, 101838.
766 <https://doi.org/10.1016/j.marmicro.2020.101838>

767 Robles, M., Peyron, O., Ménot, G., Brugiapaglia, E., Wulf, S., Appelt, O., Blache, M.,
768 Vannièrè, B., Dugerdil, L., Paura, B., Ansanay-Alex, S., Cromartie, A., Charlet, L.,
769 Guédron, S., de Beaulieu, J.-L., Joannin, S., 2023. Climate changes during the Late

770 Glacial in southern Europe: new insights based on pollen and brGDGTs of Lake Matese
771 in Italy. *Clim. Past* 19, 493–515. <https://doi.org/10.5194/cp-19-493-2023>

772 Seager, R., Liu, H., Henderson, N., Simpson, I., Kelley, C., Shaw, T., Kushnir, Y., Ting, M.,
773 2014. Causes of Increasing Aridification of the Mediterranean Region in Response to
774 Rising Greenhouse Gases*. *Journal of Climate* 27, 4655–4676.
775 <https://doi.org/10.1175/JCLI-D-13-00446.1>

776 Samartin, S., Heiri, O., Joos, F., Renssen, H., Franke, J., Brönnimann, S., Tinner, W., 2017.
777 Warm Mediterranean mid-Holocene summers inferred from fossil midge assemblages.
778 *Nature Geosci* 10, 207–212. <https://doi.org/10.1038/ngeo2891>

779 Song, B., Zhang, K., Farnsworth, A., Ji, J., Algeo, T.J., Li, X., Xu, Y., Yang, Y., 2022.
780 Application of ostracod-based carbonate clumped-isotope thermometry to paleo-
781 elevation reconstruction in a hydrologically complex setting: A case study from the
782 northern Tibetan Plateau. *Gondwana Research* 107, 73–83.
783 <https://doi.org/10.1016/j.gr.2022.02.014>

784 Tarutani, T., Clayton, R.N., Mayeda, T.K., 1969. The effect of polymorphism and magnesium
785 substitution on oxygen isotope fractionation between calcium carbonate and water.
786 *Geochimica et Cosmochimica Acta* 33, 987–996. [https://doi.org/10.1016/0016-](https://doi.org/10.1016/0016-7037(69)90108-2)
787 7037(69)90108-2

788 Toney, J.L., García-Alix, A., Jiménez-Moreno, G., Anderson, R.S., Moossen, H., Seki, O.,
789 2020. New insights into Holocene hydrology and temperature from lipid biomarkers in
790 western Mediterranean alpine wetlands. *Quaternary Science Reviews* 240, 106395.
791 <https://doi.org/10.1016/j.quascirev.2020.106395>

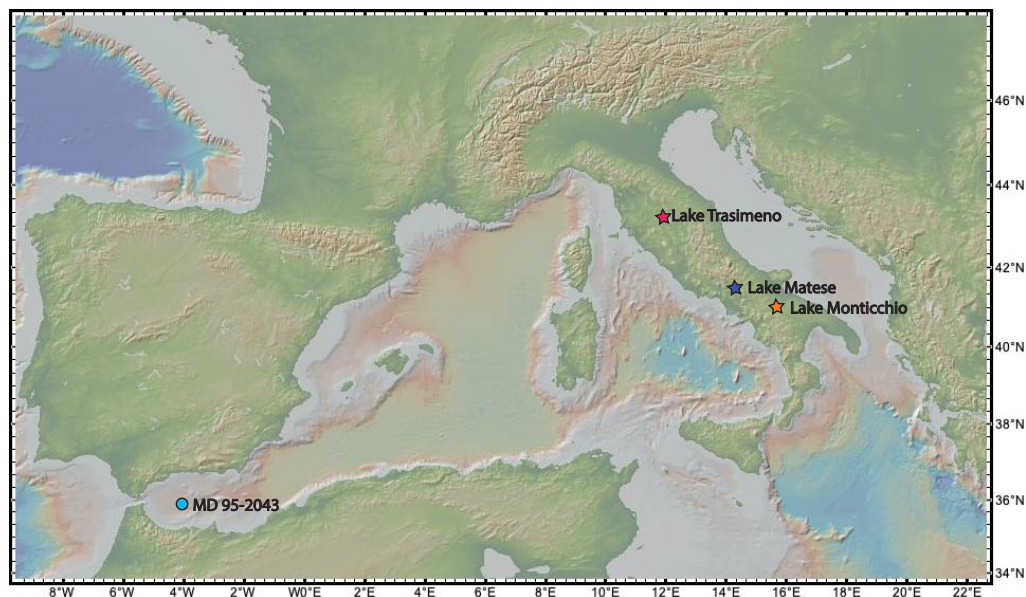
792 Turpen, J.B., Angell R.W., 1971. Aspects of moulting and calcification in the ostracode
793 *Heterocypris*. *The Biological Bulletin* 140, 331–338.

794 Yue, J., Xiao, J., Wang, X., Meckler, A.N., Modestou, S.E., Fan, J., 2022. “Cold and wet” and
795 “warm and dry” climate transitions at the East Asian summer monsoon boundary during
796 the last deglaciation. *Quaternary Science Reviews* 295, 107767.
797 <https://doi.org/10.1016/j.quascirev.2022.107767>

798 World Lake Database 2013, International Lake Environment Committee Foundation.
799 <https://wldb.ilec.or.jp>

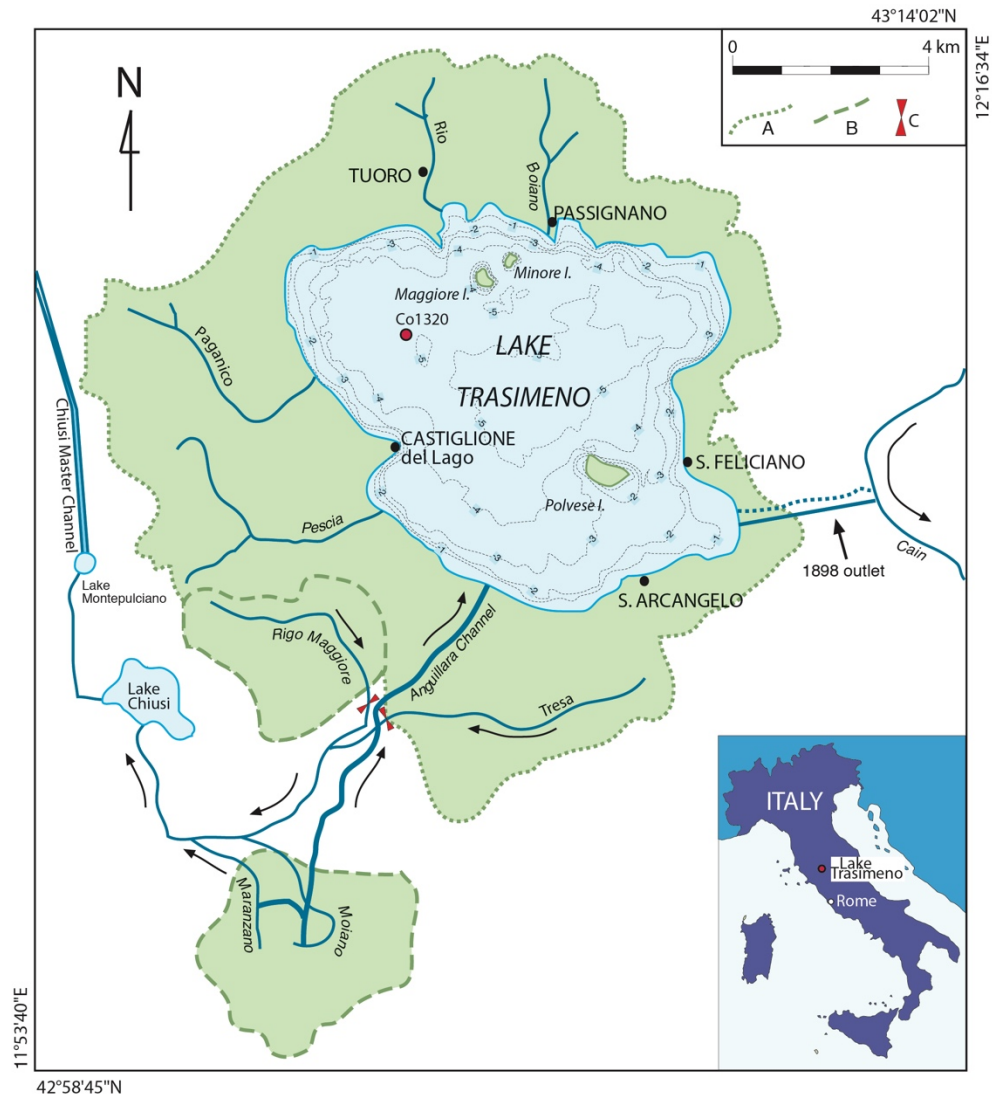
800

801 **FIGURE AND TABLE CAPTIONS**



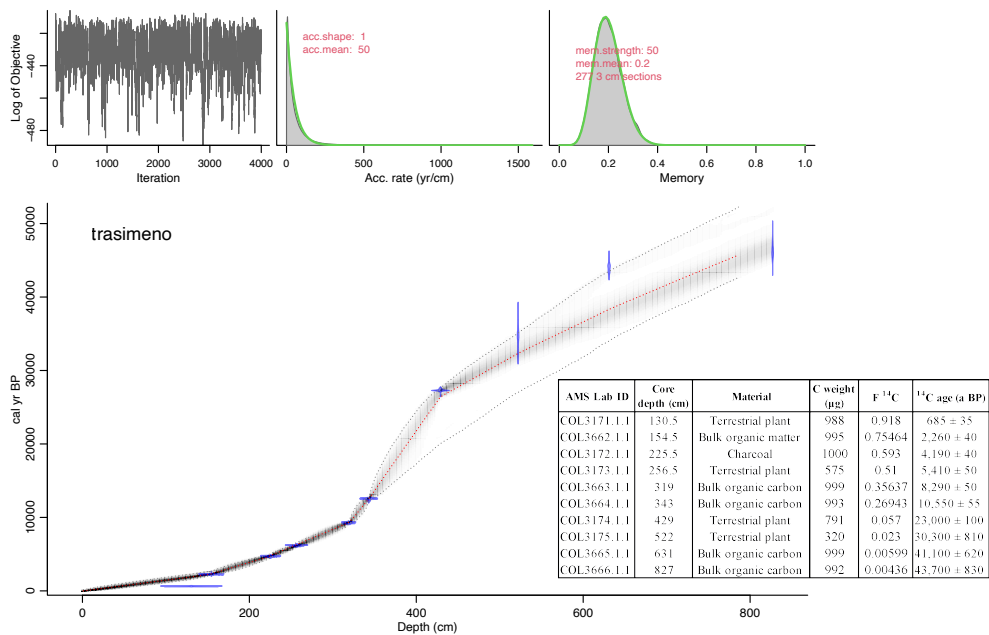
802

803 Fig. 1: Location of the records discussed in this study. Marine record MD 95-2043 from
804 Alboran Sea (Cacho et al., 1999). Lacustrine records from Lake Trasimeno (this study), Lake
805 Matese (Robles et al., 2023) and Lake Monticchio (Allen et al., 1999)



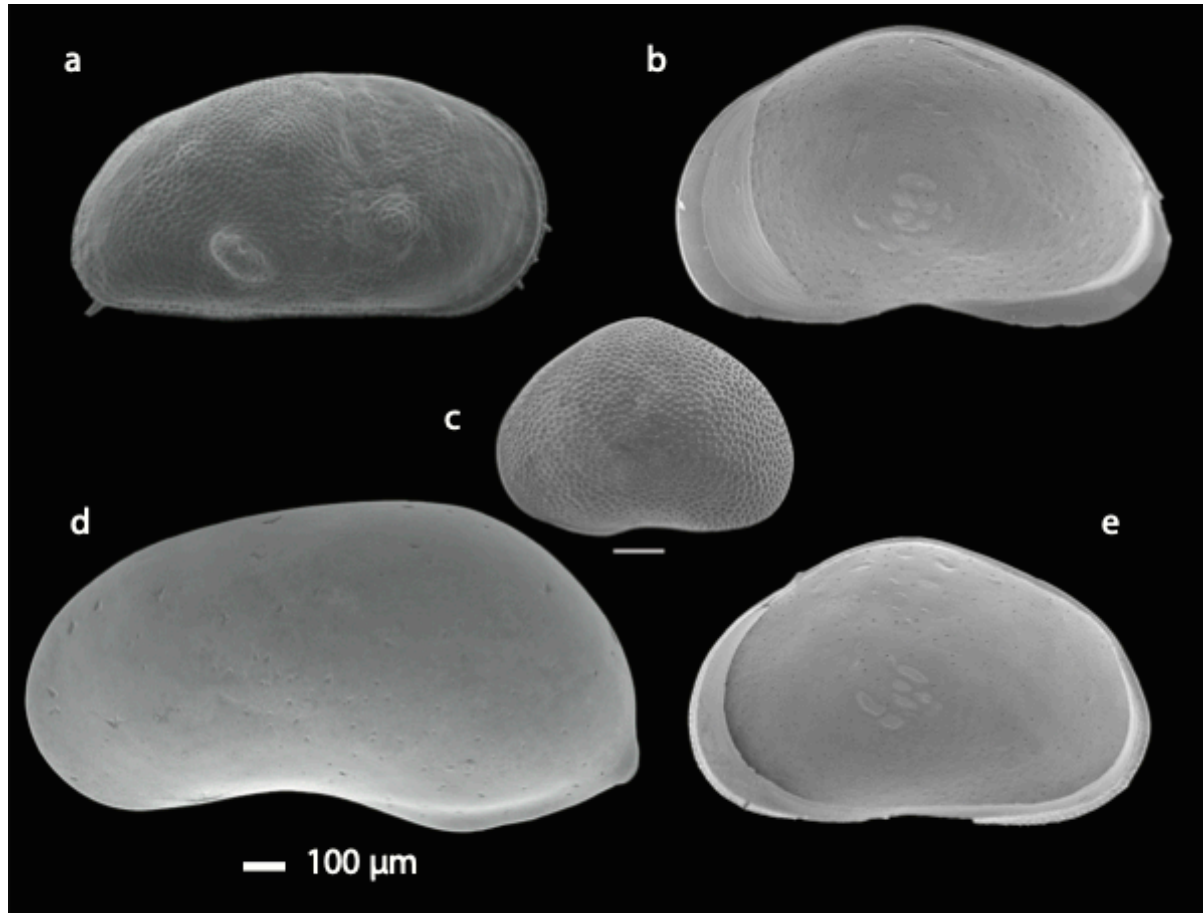
806

807 Fig. 2: Lake Trasimeno and core location, modified from Marchegiano et al. (2018).

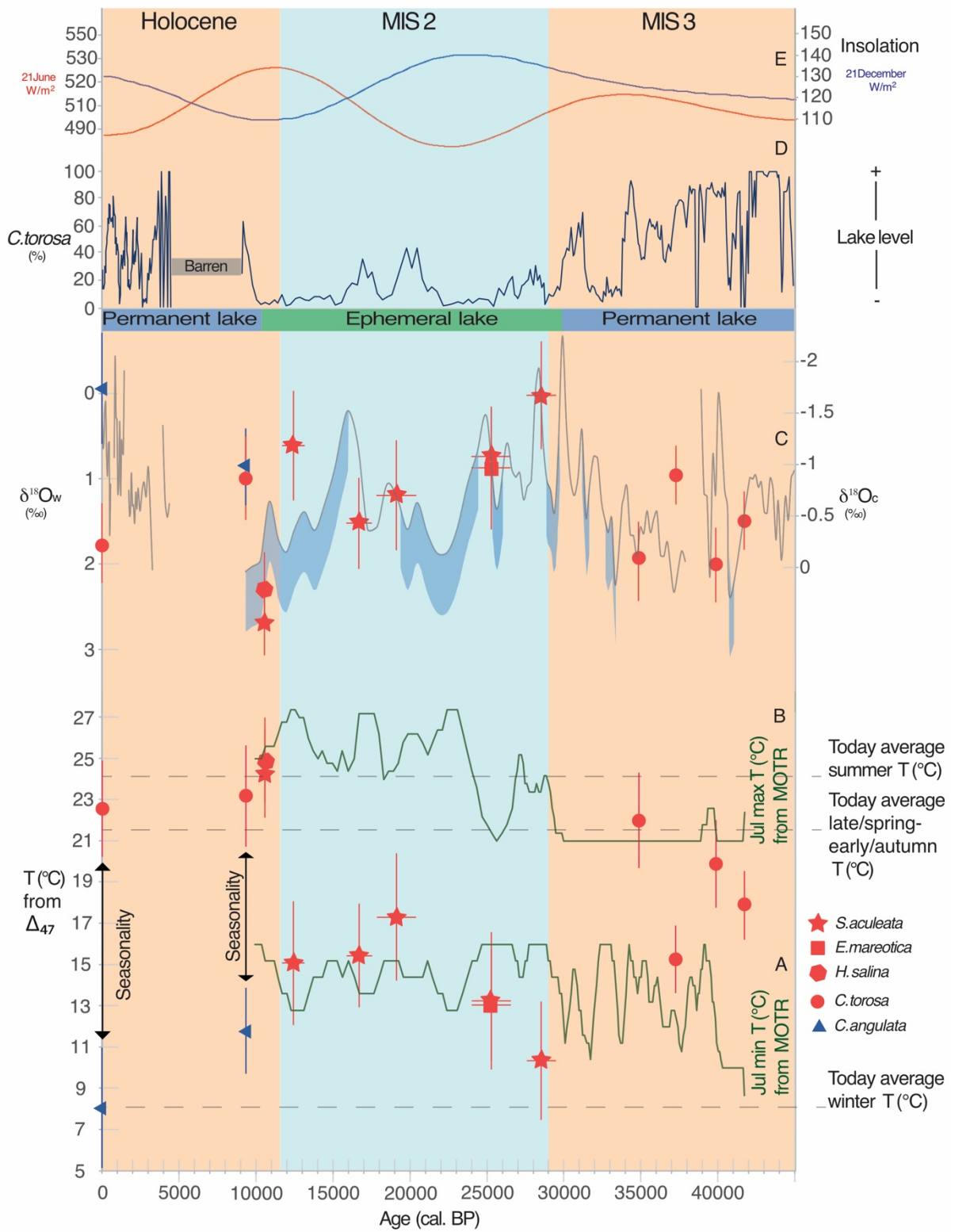


808

809 Fig. 3: Chronology of the Trasimeno core. The chronology is based on radiocarbon ages from
810 Marchegiano et al., (2018) modelled with Bayesian statistics using Bacon 3.1 0 by Blaauw &
811 Christen (2011) and IntCal 2020 (Reimer et al. 2020).



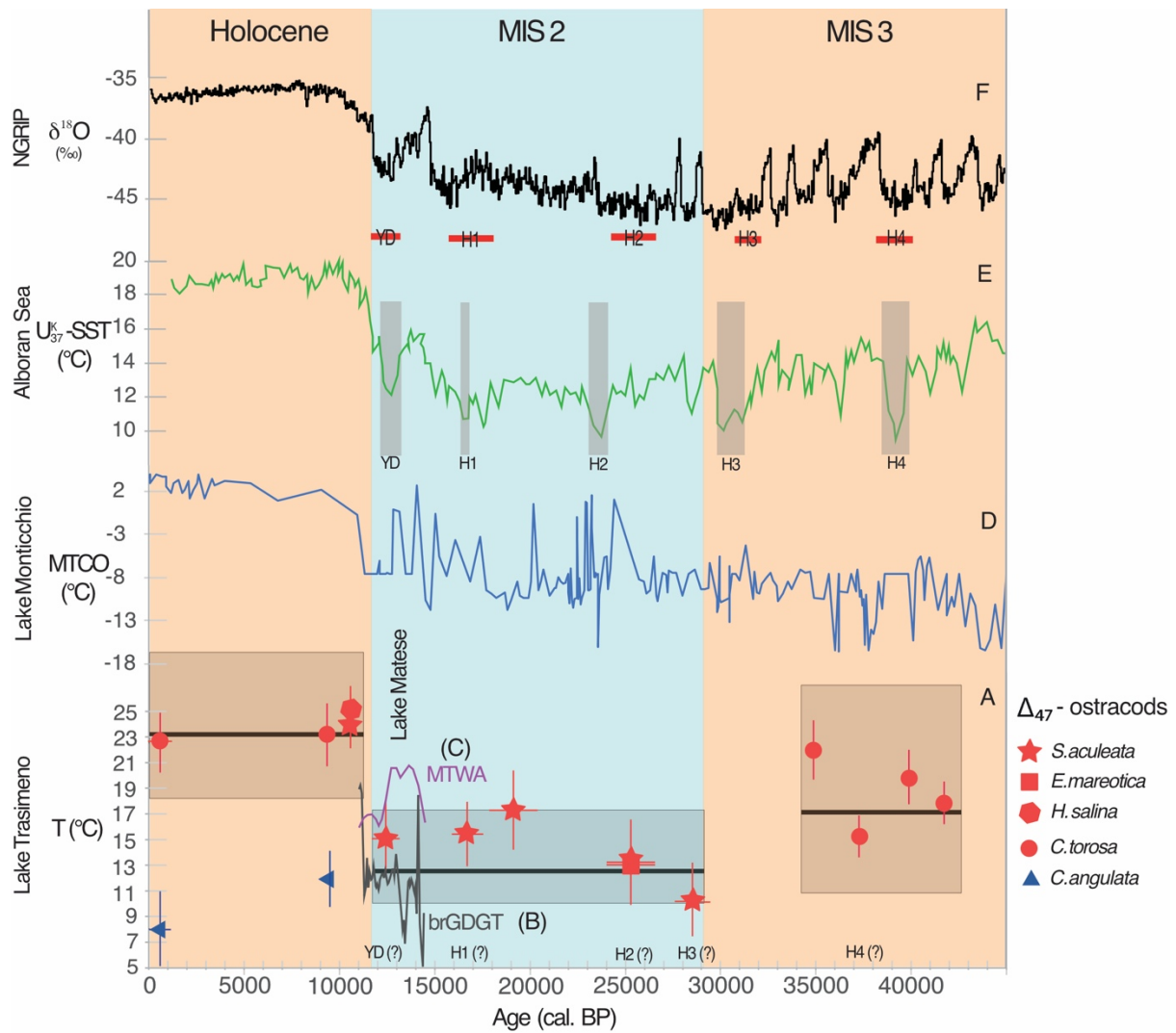
812
813 Fig. 4: Ostracod SEM pictures, made at the University of Roma Tre, obtained from samples of
814 the Lago Trasimeno Co1320 core, a. *Cyprideis torosa*, b, *Eucypris mareotica*, c,
815 *Sarcypridopsis aculeata*, d, *Candonangulata* and e, *Heterocypris salina*.



816

817 Fig. 5: Clumped isotope temperature and reconstructed $\delta^{18}\text{O}_w$ (this study) from the most
 818 abundant species *Cyprideis torosa*, *Eucypris mareotica*, *Sarocypridopsis aculeata*, *Candona*

819 *angulata* and *Heterocypris salina* (red and blue symbols: red symbols, warm season species;
820 blue symbols, cold season species). Mutual Ostracod Temperature Range (MOTR, from
821 Marchegiano et al., 2020) A (Jul min) and B (Jul max) curves, bulk carbonate $\delta^{18}\text{O}$ data of
822 Lago Trasimeno from Francke et al. (2022) (C black line,), the uncertainty in certain carbonate
823 samples (blue shade) is due to the mixed composition of aragonite/calcite and the subsequent
824 application of different correction factors (+0.6 for the aragonite, Tarutani et al., 1969)
825 (Francke et al., 2022); $\delta^{18}\text{O}_w$ reconstructed from ostracod shells (red and blue symbols: red
826 symbols, warm season species; blue symbols, cold season species), *C. torosa* ostracod
827 abundance used to reconstruct lake level variations (D curve) (Marchegiano et al., 2018) and
828 summer and winter insolation (E curve) (Laskar et al., 2004). Present mean water winter, late
829 spring/early autumn and summer temperature are indicated.



830

831 Fig. 6: Paleotemperature reconstruction at Lake Trasimeno and comparison with other
 832 Mediterranean records (A). Box plots for Δ_{47} temperatures, including all replicate
 833 measurements per each samples (see Table 1 in supplementary material), show median (black
 834 bold line), the first (25%) and third quartiles (75%, i.e. the grey box covers 50% of the
 835 probability density function) (A), brGDGT mean annual (B) and pollen reconstructed mean
 836 temperatures of the warmest month (MTWA) (C) from Lake Matese (Robles et al., 2023),
 837 pollen reconstructed mean temperatures of the coldest month (MTCO) from Lake Monticchio
 838 (D) (Allen et al., 1999) alkenones marine surface annual mean temperature from Alboran Sea
 839 (E) (Cacho et al., 1999) and the $\delta^{18}\text{O}$ from the North Greenland Ice Core Project (F)
 840 (Rasmussen et al., 2016).

Sample name	Depth (cm)	n°. replicates	$\Delta 47$ (‰)	$\Delta 47$ SE	$\Delta 47$ -T	d13C (‰)	d18O (‰)	Specie	Vital offset (‰)	d18Ocorr (‰) (VPDB)	d18Ow (‰)	d18Ow SE	Average age (ky. cal BP)	Age
TRAR1	14-83	6	0.6485	0.0144	8.0	-0.49	3.13	<i>C. angulata</i>	-2.2	0.93	-0.0596	0.326	0.7	HOLOCENE
TRAR2	14-83	10	0.6012	0.0111	22.5	-3.17	0.42	<i>C. torosa</i>	-0.8	-0.38	1.7554	0.234	0.7	
TRAHOL1	316-322	9	0.5993	0.0115	23.2	-0.28	-0.45	<i>C. torosa</i>	-0.8	-1.25	0.9891	0.248	9	
TRAHOL2	316-322	10	0.6356	0.0111	11.8	2.17	3.2	<i>C. angulata</i>	-2.2	1	0.8604	0.226	9	
TRA2	328-330	12	0.5941	0.0101	24.9	3.99	0.03	<i>S. aculeata</i>	0	0.03	2.6674	0.202	10.5	
TRA2B	328-330	11	0.596	0.0105	24.3	3.6	-0.21	<i>H. salina</i>	0	-0.21	2.2886	0.215	10.5	
TRAGI1	336-348	6	0.6247	0.014	15.1	2.54	0.055	<i>S. aculeata</i>	0	0.055	0.6114	0.321	12	LGM-MIS2
TRAH1	363-375	8	0.6235	0.0123	15.4	3.5	0.86	<i>S. aculeata</i>	0	0.86	1.5216	0.267	17	
TRAGS2	375-393	6	0.6175	0.014	17.3	3.58	0.15	<i>S. aculeata</i>	0	0.15	1.1930	0.323	19	
TRAH2-1	413-431	7	0.6314	0.0131	13.0	3.09	0.61	<i>S. aculeata</i>	0	0.61	0.7368	0.290	25	
TRAH2-2	413-431	5	0.6307	0.0153	13.2	1.7	0.696	<i>E. mareotica</i>	0	0.696	0.8720	0.360	25	
LATEMIS3	445-477	6	0.6405	0.014	10.3	0.1	0.5	<i>S. aculeata</i>	0	0.5	0.0215	0.316	28	
TRA4	561-569	10	0.6029	0.0111	22.0	-1.32	0.74	<i>C. torosa</i>	-0.8	-0.06	1.9688	0.233	35	BLGM-MIS3
TRA5	603-616	14	0.6241	0.0094	15.2	-0.47	1.15	<i>C. torosa</i>	-0.8	0.35	0.9557	0.173	37	
TRA6	658-654	11	0.6094	0.0107	19.9	0.64	1.21	<i>C. torosa</i>	-0.8	0.41	2.0096	0.219	40	
TRA7	732-748	14	0.6157	0.0093	17.9	-3.47	1.12	<i>C. torosa</i>	-0.8	0.32	1.4897	0.171	42	

841

842 Table 1: Carbonate classic and clumped isotopes results. The $\Delta 47$ -T are calculated using the
843 unified calibration (Anderson et al., 2021) and the $\delta^{18}O_w$ calculated from $\Delta 47$ and $\delta^{18}O_{ost}$ data
844 using the formula of Kim and O'Neal (1997). BLGM: Before Last Glacial Maximum; LGM:
845 Last Glacial Maximum.

SPECIES	CALCIFICATION SEASON	AGE	SAMPLE	$\Delta 47$ -T (2SE)	TODAY AVERAGE SEASON WATER-T
<i>C. torosa</i>	late-spring/early-autumn	HOLOCENE	TRAR2	22,5 ± 2.3	21.4
			TRAHOL1	23,1 ± 2.5	21.4
		BLGM-MIS3	TRA4	22 ± 2.3	21.4
			TRA5	15,2 ± 1.6	21.4
			TRA6	19,9 ± 2.1	21.4
			TRA7	17,9 ± 1.7	21.4
<i>S. aculeata</i>	summer	HOLOCENE	TRA2	24,9 ± 2	24
		LGM-MIS2	TRAGI1	15,1 ± 3	24
			TRAH1	15,4 ± 2.5	24
			TRAGS2	17,3 ± 3.1	24
			TRAH2-1	13,0 ± 2.7	24
LATEMIS3	10,3 ± 2.9	24			
<i>E. mareotica</i>	summer	LGM-MIS2	TRAH2-2	13,2 ± 3.3	24
<i>H. salina</i>	summer	HOLOCENE	TRA2B	24,3 ± 2.2	24
<i>C. angulata</i>	winter	HOLOCENE	TRAR1	8 ± 2.9	8
			TRAHOL2	11,8 ± 2.1	8

846

847 Table 2: Ostracod species used for $\Delta_{47} - T$ reconstruction, their shell calcification season (*C.*
848 *torosa*, from Heip, 1976, Roberts et al., 2020 and consideration from this study; *S. aculeata*
849 Meisch et al., 2000; *E. mareotica*, Li and Liu, 2010; *H. salina*, Meisch et al., 2000; *C.*
850 *angulata*, Meisch et al., 2000) and present average seasonal Lake Trasimeno water
851 temperatures (World Lake database 2023)